REMARKS/ARGUMENTS

Favorable reconsideration of this application, in light of the following discussion, is respectfully requested.

Claims 1-6, 8, 9, 12-17, 21-26, and 28-35 are pending in the present application,

In the outstanding Office Action, Claims 1-3, 5, 9, 16, 17, and 28-30 were rejected under 35 U.S.C. §102(e) as anticipated by Leung et al. (U.S. Patent No. 6,653,718, hereinafter Leung); Claims 4, 6, and 26 were rejected under 35 U.S.C. §103(a) as unpatentable over Leung in view of Gu et al. (U.S. Patent No. 6,551,901, hereinafter Gu); Claims 8, 12-15, 21-25, 31, 33, and 35 were allowed; and Claims 32 and 34 were objected to from depending from a rejected base claim, but were otherwise indicated as including allowable subject matter.

Applicants thank the Examiner for the courtesy of an interview extended to Applicants' representatives on June 9, 2006. During the interview, differences between the present invention and the applied art, and the rejections noted in the outstanding Office Action were discussed. The Examiner acknowledged that Stober (which is incorporated by reference into Leung) does not disclose the range of the average diameter of the insulating particles in Claim 1, and that the outstanding rejection would be withdrawn after a response is filed. Arguments presented during the interview are reiterated below.

Applicants also thank the Examiner for the indication that Claims 8, 12-15, 21-25, 31, and 35 are allowed and that Claims 32 and 34 include allowable subject matter. Applicants note that Claim 9 depends from allowed Claim 8. Thus, Applicants respectfully request that the rejection of Claim 9 be withdrawn.

With respect to the rejection of Claim 1 under 35 U.S.C. §102(e) as anticipated by Leung, Applicants respectfully traverse this ground of rejection. Amended Claim 1 recites *inter alia*, "wherein an average diameter of the insulating particles falls within a range of 100

nm to 500 nm or a range of 100 nm to half a width of opening of the trench." Leung does not describe or suggest at least this element of amended Claim 1.

During the above-noted interview, the Examiner indicated that he was relying on Stober (U.S. Patent No. 3,634,558), which is incorporated by reference into Leung, to disclose the above-noted claim element.

Col. 4, lines 55-57 of Stober discloses particles with diameters between 1.5 and 2 μ (or 1500 nm to 2000 nm). This is clearly greater than the claimed range of 100 nm to 500 nm.

Leung also incorporates by reference *Preparation and Characterization of Spherical Mondisperse Silica Dispersions in Nonaqueous Solvents*, by Helden et al. (hereinafter Helden). As a courtesy, a copy of this reference is submitted herewith.

Applicants respectfully submit that Helden does not cure the above-noted deficiencies in Leung and Stober. Helden discusses the preparation of silica dispersions in alcohol. Helden is not directed toward a semiconductor device, and does not disclose or suggest a semiconductor device that includes "a particulate insulating layer filling at least a lower portion of the trench and comprising insulating particles, wherein an average diameter of the insulating particles falls within a range of 100 nm to 500 nm or a range of 100 nm to half a width of opening of the trench."

Leung, at col. 3, lines 31-33 and col. 4, lines 40-45, describes that particles having a diameter equal to or larger than 100 nm are excluded. The purpose of the small insulating particles in Leung is to fill gaps smaller than 100 nm.[1] Particles larger than 100 nm are unfit for the semiconductor device of Leung.

MPEP §2163.07(b) states "The information incorporated is as much a part of the application as filed as if the text was repeated in the application, and should be treated as part

[1] Leung, col. 8, lines 60-63, and col. 1, lines 21-25.

of the text of the application as filed." However, Applicant notes MPEP §2141.02(VI), which states "[a] prior art reference must be considered in its entirety, i.e., as a whole, including portions that would lead away from the claimed invention. *W.L. Gore & Associates, Inc. v. Garlock, Inc.*, 721 F.2d 1540, 220 USPQ 303 (Fed. Cir. 1983), *cert. denied*, 469 U.S. 851 (1984)."

As a whole, Leung excludes particles greater than 100 nm, and the disclosure of Helden is merely intended to add an explanation of how to make the smaller than 100 nm particles.

Furthermore, MPEP §2131 states "The identical invention must be shown in as complete detail as is contained in the ... claim." *Richardson v. Suzuki Motor Co.*, 868 F.2d 1226, 1236, 9 USPQ2d 1913, 1920 (Fed. Cir. 1989). The elements must be arranged as required by the claim, but this is not an *ipsissimis verbis* test, i.e., identity of terminology is not required. *In re Bond*, 910 F.2d 831, 15 USPQ2d 1566 (Fed. Cir. 1990)." Since Leung discloses that particles with a diameter greater than or equal to 100 nm are excluded from the particulate insulating layer of the semiconductor device, Applicants respectfully submit that a person of ordinary skill in the art would not read the combined disclosures of Leung and Helden as disclosing the claimed "wherein an average diameter of the insulating particles falls within a range of 100 nm to 500 nm or a range of 100 nm to half a width of opening of the trench."

Furthermore, Applicants respectfully submit that a rejection under 35 U.S.C §102 is improper because the semiconductor device of Leung would have to be modified to disclose the claimed invention in as much detail as claimed. A proper rejection would be under 35 U.S.C. §103(a), and include an explanation, supported by evidence on the record, as to why a person of ordinary skill in the art would modify the semiconductor device of Leung to

include insulating particles with a diameter in the range of 100 nm to 500 nm or 100 nm to half a width of opening of the trench.

Because Leung, even when considered along with the disclosure of Helden, does not disclose or suggest the identical invention in as complete detail as contained in Claim 1, Applicants respectfully submit that Claim 1 patentably distinguishes over Leung.

Furthermore, Applicants respectfully submit that Gu does not cure the above-noted deficiencies in Leung.

In view of the above-noted distinction, Applicants respectfully submit that amended Claim 1 (and Claims 2-6 dependent thereon) patentably distinguish over Leung and Gu, taken alone or in proper combination. Applicants respectfully submit that Claim 16 is similar to Claim 1. Thus, Applicants respectfully submit that Claim 16 (and Claims 17 and 30 dependent thereon) patentably distinguish over Leung and Gu, taken alone or in proper combination, for at least the reasons stated for Claim 1.

Consequently, in light of the above discussion, the present application is believed to be in condition for allowance and an early and favorable action to that effect is respectfully requested.

Respectfully submitted,

OBLON, SPIVAK, McCLELLAND,
MAIER & NEUSTADT, P.C.

Eckhard H. Kuesters
Attorney of Record
Registration No. 28,870

Joseph Wrkich
Registration No. 53,796

Surinder Sachar
Registration No. 34,423

Customer Number
22850

Tel: (703) 413-3000
Fax: (703) 413 -2220
(OSMMN 06/04)

I:\ATTY\JW\244619US\244619US_AM DUE 6-29-06.DOC

Preparation and Characterization of Spherical Monodisperse Silica Dispersions in Nonaqueous Solvents

A. K. VAN HELDEN, J. W. JANSEN, AND A. VRIJ

Van't Hoff Laboratory for Physical and Colloid Chemistry, Transitorium III, Padualaan 8, 3584 CH Utrecht, The Netherlands

Received June 16, 1980; accepted October 13, 1980

In two earlier papers (A. K. van Helden and A. Vrij, *J. Colloid Interface Sci.* **76**, 418 (1980); **78**, 312 (1980)) light-scattering measurements of organophilic silica dispersions were reported. The preparation of these dispersions is described here in more detail. Organophilic silica dispersions consisting of spherical particles of narrow size distribution were produced by a combination of two earlier described processes. First uniform silica particles were prepared by hydrolysis of ethylorthosilicate according to the method of W. Stöber A. Fink, and E. Bohn (*J. Colloid Interface Sci.* **26**, 62 (1968)). Then these particles were rendered organophilic by a coating reaction with stearyl alcohol according to R. K. Iler's method (U. S. Patent 2,801,185). Stable dispersions with particle radius between 20 and 100 nm were prepared in various organic solvents, e.g., cyclohexane, *n*-octane, diethylether. The stability does not reduce upon storage in cyclohexane for more than 1 year. A range of systems is investigated with a number of common techniques in colloid research, e.g., electron microscopy, ultracentrifugation, static and dynamic light scattering. The results can be qualitatively explained in terms of an initially porous alcosol particle which is dehydrated to some extent in the coating reaction. At low concentrations especially in diethylether electrostatic repulsion seems to occur. At higher concentrations this effect is not observed (van Helden and Vrij, *J. Colloid Interface Sci.* **78**, 312 (1980)).

I. INTRODUCTION

Colloidal particles with well-defined size and shape and with narrow size distribution are of great importance in studies of concentrated colloidal dispersions. It is our purpose to perform experiments with various kinds of particles—in particular in nonpolar solvents—and to interpret their behavior in terms of fluid state theories (1). We studied the light scattering of PMMA latices (2) and microemulsions (3) in benzene and more recently organophilic silica (4, 5) in cyclohexane.

Among the large number of well defined inorganic dispersions that were recently discovered (6) silica was chosen for several reasons:

(a) The refractive indices of amorphous silica and nonpolar liquids like chloroform and cyclohexane are rather close together so that multiple scattering can be minimized.

(b) Stöber (7) reported a very elegant method of preparing monodisperse spherical silica particles with sizes covering almost the whole colloidal range.

(c) Colloidal silica was intensively investigated in the last decades (8). In particular, a number of ways are known to render silica organophilic by coating the surface with small organic molecules, e.g., alkyl silanol compounds (8, 9). More recently it was also shown that polymeric chains could be attached to silica particles either by deactivation of living polymer at the surface, e.g. (10), or by growing chains from initiating groups at the surface (11).

Among the methods of surface modification we preferred the esterification with alcohols, because this method seemed experimentally relatively easy. In particular

0021-9797/81/060354-15$02.00/0

it could be easily applied in conjunction with the silica sols in alcohol (alcosols), obtained according to Stöber's method. The Si–O–C bond, formed after esterification with an alcohol, is chemically less stable against hydrolysis than the Si–O–Si bond, which is formed after reaction with silanes. Deuel *et al.* (12) showed, however, that the stability is satisfactory with large organic groups and dense surface coverage.

In this paper we shall report more extensively than in (4) and (5) on our preparation of organophilic silica, and we shall go into more detail upon the characterization of these systems. Because this type of organophilic silica is not only important as a model system but might also find technical application (13), it seems expedient to us to include results of a larger range of investigated systems. This accumulation of experimental data, however, must necessarily be considered as incomplete and partly preliminary.

II. EXPERIMENTAL

1. Materials

Absolute ethanol (Baker) and ammonium hydroxide, 25% (Merck) were of analytical reagent quality. Titrations indicated an ammonia concentration of 14.2 moles dm^{-3}. Ethylorthosilicate (Fluka) was of purum grade. Absolute ethanol and ethylorthosilicate were distilled immediately before use. Stearyl alcohol was supplied by Merck (technical grade) and Lameris (99.5%), and used without further purification.

2. Characterization Techniques

Transmission electron microscope measurements were performed with a Philips EM 301 apparatus. Carrier grids covered with carbon-coated Parlodion films were dipped in a dilute dispersion and electron micrographs were taken of the particles retained on the film. Accurate results were obtained by prior calibration with grating replicas.

Light-scattering intensity and light-scattering fluctuation spectroscopy and refractive index increment measurements were performed as previously (4).

Small-angle X-ray (SAXS) measurements were performed with a Kratky camera. The scattered intensity (Cu$K\alpha$ radiation) was registrated photographically at diffraction angles between 0.00049 and 0.077 radians.

Sedimentation velocity experiments were carried out in a Beckman Spinco (model E) analytical ultracentrifuge, using a 12-mm standard single-sector cell and an AN-D rotor at temperatures between 23 and 25°C. A series of consecutive pictures was taken of the Schlieren image of the samples.

Density measurements were conducted at 25.10°C with a Precision Density Meter DMA O2C (Anton Paar KG, Austria).

Surface area determinations were carried out by physisorption of nitrogen at 77°K with a Carlo-Erba sorptometric apparatus.

The carbon and hydrogen content of the silica was determined gravimetrically. The sample was combusted at 800°C and the carbon dioxide and water were adsorbed. The silicon was determined as residual ash after pretreatment with H_2SO_4 and HNO_3 combustion at 850°C.

3. Alcosol Preparation

Silica dispersions in alcohol (here called alcosols) were prepared according to the method of Stöber (7). Ethylorthosilicate is hydrolyzed in a mixture of alcohol, ammonia, and water. Two types of reactions occur in the formation of silica particles. Silanol groups are formed by hydrolysis and siloxane bridges are formed by a condensation polymerization reaction. Spherical particles are obtained when enough ammonia is present in the initial reaction mixture. The final particle size depends mainly on the initial water and ammonia concentration.

Glassware was cleaned with 2% hydrogen fluoride, rinsed with distilled water and absolute ethanol. Ammonium hydroxide

and absolute ethanol were mixed in the reaction vessel. Then ethylorthosilicate was added and the reaction mixture was stirred at ambient temperature for 18 hours. The total amount of solution varied between 0.2 and 3 liters. After an (invisible) hydrolytic reaction, in which silicic acid is formed, the condensation reaction of the supersaturated silicic acid was indicated by an increasing opalescence of the mixture starting 0.5–2 hours after adding ethylorthosilicate. No further change in turbidity was observed after 10 hours indicating that the final particle size was reached. In different experiments the particle size was reproduced within 20%. The opalescence of the alcosols did not change for at least a few months. After 1 year the turbidity markedly increased, probably due to aggregation of particles.

4. *Organophilic Silica Sols*

Iler (14) reported a method of preparing organophilic silica by esterification of surface silanol groups with alcohols. To an aqueous silica sol he added a water-miscible alcohol and removed the water by distillation. Then the substantially anhydrous alcosol was heated to at least 100°C to effect surface esterification. Ballard *et al.* (15) showed that the degree of esterification increases with reaction time and temperature. He found for stearyl alcohol that a dense layer of aliphatic chains is formed when the reaction is carried out at 200°C for 3 hours.

With the Stöber process the silica is directly prepared in a lower alcohol (in our case ethanol). The reaction with higher alcohols can be performed by simply adding it to the alcosol and distilling the lower alcohol. Preferably stearyl alcohol is added as a concentrated solution in ethanol. The amount of stearyl alcohol was 3–5 times the silica weight. When necessary the water concentration in the beginning of the ethanol distillation was lowered to 4.4% by dilution with absolute ethanol in order to remove the water from the dispersion during the distillation process. Then the silica was esterified with stearyl alcohol at 180–200°C for 3 hours under nitrogen atmosphere. The silica was readily dispersable in cyclohexane, *n*-alkanes, chloroform, and toluene. Stable dispersions were also obtained after esterification at 200°C for 40 min, and the stability did not change after prolonged heating (9 hours).

5. *Purification of Sols*

The separation of the silica from the large excess stearyl alcohol was achieved by a combination of vacuum distillation/sedimentation or by a combination of nitrogen flow distillation/sedimentation or by sedimentation alone. In the nitrogen flow distillation, nitrogen gas is blown over the stearyl alcohol melt containing the silica (180°C). The stearyl alcohol vapor is carried along and crystallizes in the condenser. After distillation the silica was dispersed in cyclohexane and sedimentated in a preparative ultracentrifuge (18,000 rpm). The supernatant with remaining stearyl alcohol was discarded. When the purification is performed by sedimentation alone the stearyl alcohol melt with silica was dissolved in a mixture of chloroform (60% v/v) and cyclohexane (40% v/v). Chloroform is used because it is a good solvent for stearyl alcohol. Cyclohexane is added in order to increase the density difference of particle and medium, thereby increasing the sedimentation velocity. The supernatant was again discarded and the silica sediment dispersed in cyclohexane. Two additional sedimentation runs in cyclohexane were then carried out to remove all stearyl alcohol.

When the organophilic silica was stored in concentrated dispersions in cyclohexane, the appearance was not changed after more than 2 years. The coated silica can be dried at 80°C for 24 hours under nitrogen atmosphere without affecting its organophilic properties. Prolonged storage in air, how-

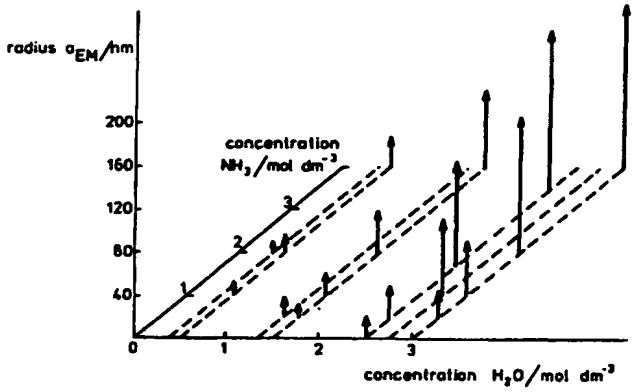

FIG. 1. Radius of silica particles in alcosols as a function of initial water and ammonia concentration determined with electron microscopy (three-dimensional plot). The ethylorthosilicate concentration was 0.17 mole dm^{-3}. The arrows indicate the lengths of the particle radii.

ever, deteriorates its organophilic nature, probably due to hydrolysis or oxidation of the coating layer.

III. RESULTS

1. Alcosols

Some preliminary alcosol preparations were performed in order to check the influence of the ammonia and water concentration on the final particle size. Because we were particularly interested in particles in the range 10–100 nm, the ammonia concentration was chosen below 4 moles dm^{-3} and the water concentration below 3 moles dm^{-3}, in agreement with Stöber's recipe. The ethylorthosilicate concentration was 0.17 mole dm^{-3}. The results of particle size determinations with electron microscopy are shown in Fig. 1. The particle size was found to increase with increasing water and ammonia concentration. The particle radius, a_{EM}, varied between 10 and 150 nm. (According to Stöber even particles with a radius of 500 nm can be obtained at still higher concentrations of water and ammonia.)

From the electron micrographs we also determined the particle size distribution as a function of average particle size. The standard deviation, Δ, expressed as a percentage of the mean radius is shown in Fig. 2. It decreases slightly with increasing particle size.

The influence of increasing initial ethylorthosilicate concentration was investigated at 0.82 mole dm^{-3} ammonia and 2.5 moles dm^{-3} water: a_{EM} tends to decrease, whereas Δ increases. The particle shape becomes progressively irregular when the ethylorthosilicate concentration exceeds 0.2 mole dm^{-3}. In our further experiments we always used concentrations between 0.14 and 0.20 mole dm^{-3}.

Three dilute alcosols were also investigated with small-angle X-ray scattering. Differential volume distributions were determined according to Vonk (16) (method I). The results are presented in Fig. 3. Notice the high peak at $a \simeq 1$ nm. It is not clear whether this peak originates from data processing artifacts, or from real particle inhomogeneities with a short correlation length. From the right-hand-side peaks the standard deviation in the volume distribution curve was determined. This parameter is comparable with Δ since the distribution is narrow. In Fig. 2 values of the standard deviation determined with SAXS are also shown. They are in reasonable agreement with the EM results.

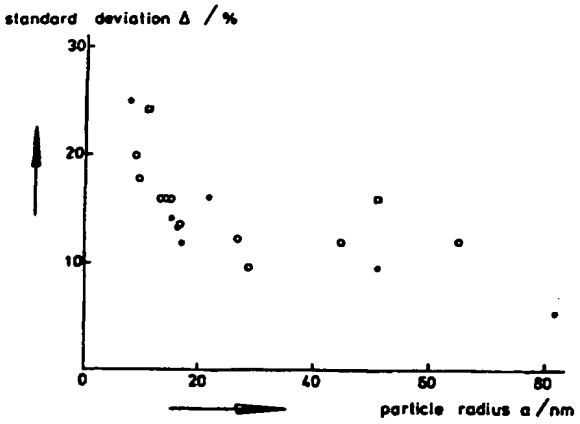

FIG. 2. Standard deviation in the size of SiO_2 particles in alcosols as a function of particle size, determined with electron microscopy (○), and with small-angle X-ray scattering (□). From electron micrographs 100–250 particles were counted. Also the results of electron micrographs of coated silica (●) are shown.

One alcosol was characterized more extensively. The sample was coded S_8^*, the asterisk denoting an *un*coated silica. We shall mention the results of element analysis, nitrogen adsorption, density measurements, and light scattering.

The silicon, hydrogen, and carbon contents of the sample were determined by element analysis after drying at 180°C for 24 hours in vacuum. We found: Si = 42.7, H = 0.75, and C = 0.80 wt%. Assuming that the carbon originates from unhydrolyzed ethoxy groups, one calculates from these data that the particles contain: 91.5% silica, 5.25% water, and 0.97% ethoxy groups.

Nitrogen adsorption was measured at 77°K, after drying the sample at 180°C in vacuum. The isotherm was analyzed according to the BET equation and with the standard de Boer *t* curve (17). Also (cumulative)

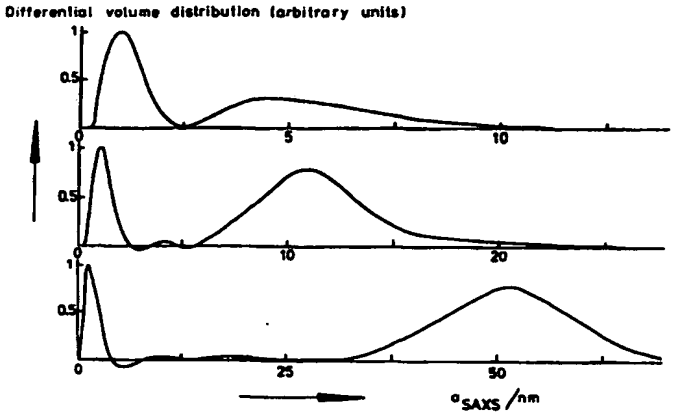

FIG. 3. Particle volume distributions in alcosols, determined with small-angle X-ray scattering.

TABLE I

Characterization of Organophilic Silicas

Sample	S_6	S_8	S_{10}	S_7	S_9
C/% (w/w)	14.68	13.05	12.66	6.15	2.82
H/% (w/w)	3.50	3.13	2.71	1.89	1.70
Si/% (w/w)	35.69	37.05	37.03	40.10	—
$S_{BET}/m^2\ g^{-1}$	—	70.8	79.1	26.2	—
$D_0/10^{-12}\ m^2\ sec^{-1}$	11.0	10.5	9.15	3.88	2.66
$s_0/10^{-11}$ sec	6.81[a]	8.34	29.4[b]	102	—
$\delta/g\ cm^{-3}$	1.61	1.65	1.73	1.78	—
$M_{SD}/10^7\ g\ mol^{-1}$	2.95	3.74	6.08	121	—
$M_{CV}/10^7\ g\ mol^{-1}$	2.6	3.4	—	110	290–390
$\bar{n}_p$ (λ_0 = 546 nm)	1.453	1.449	—	1.439	1.437–1.445
R_{gp}/nm	21	21	—	49	75
E/nm^2	—	—	—	11	31

Note. Contrast variation results of S_7 were published in Ref. (4).

[a] See Ref. (31).

[b] Measured in *n*-heptane.

surface area and pore volume were determined from the hysteresis of the adsorption and desorption isotherm according to (18). From the BET method a surface area of 268 $m^2\ g^{-1}$ was obtained. The *t*-plot analysis yielded 141 $m^2\ g^{-1}$ and the cumulative surface area was 95.5 $m^2\ g^{-1}$. The *t*-plot analysis also showed that the sample contains an appreciable amount (~0.065 $cm^3\ g^{-1}$) of ultramicropores, i.e., pores with size < 1.2 nm. In such cases the BET method overestimates the surface area and we think that the value of 268 $m^2\ g^{-1}$ is too high. The de Boer *t* curve is valid for (hydr)oxide surfaces. Our sample, however, may contain an appreciable amount of ethoxy groups at the particle surface, as indicated by the carbon content of the particles. Probably the value of 95.5 $m^2\ g^{-1}$ is the most accurate one.

The density of S_8^s was determined in a dilution series with supernatant, obtained by centrifugating another portion of alcosol. The concentration was 0–12 g dm^{-3}. The specific volume was, $\bar{v}$ = 0.534 $cm^{-3}\ g^{-1}$, which gives a density, δ = 1.87 g cm^{-3}.

A light-scattering experiment and a refractive index increment determination were performed with S_8^s diluted with supernatant. Measurements were carried out 3 months after the alcosol preparation. The refractive index increment (dn/dc) = 56.8 * 10^{-3} $cm^3\ g^{-1}$ for wavelength, λ_0 = 436 nm. The light-scattering results were interpreted with the well-known equation (19),

$$(1 + \cos^2\theta)\mathcal{K}c/R(K) = (1/M)(1 + K^2R_g^2/3)(1 + 2A_2c) \quad [1]$$

with

$$\mathcal{K} = 2\pi^2n^2(dn/dc)^2(\lambda_0^4N_A)^{-1}, \quad [2]$$

where $K = (4\pi n/\lambda_0)\sin(\theta/2)$ is the scattering wave vector, θ is the scattering angle, c the particle weight concentration, $R(K)$ the Rayleigh ratio (unpolarized light), M the particle molar mass, R_g the radius of gyration, A_2 the second virial coefficient, and N_A is Avogadro's number. We found a high value of A_2 (=1.5 * 10^2 $cm^3\ g^{-1}$), which is probably electrostatic in nature. M values were large compared with M_{SD} (see next section) but they are overestimated due to the large A_2.

2. *Organophilic Silica*

A number of organophilic silicas were characterized with element analysis, nitrogen adsorption, electron microscopy, static and dynamic light scattering, small-angle

X-ray scattering, ultracentrifugation, and density measurements. The first three methods yield information about silica particles in a dried state, whereas the latter methods refer to particles in the dispersed state. We shall report now on the results of the different methods.

2.1. Element analysis. The samples were dried at 180°C in vacuum for 24 hours. The results (see Table I) show that the carbon content is different for different particle size, compare, e.g., with the molar mass M_{SD}. The substantial carbon content indicates that aliphatic chains are present at the particle surface.

2.2. Nitrogen adsorption. From the nitrogen adsorption isotherm the surface area was determined according to the BET equation (S_{BET}). The surface area was also determined from the de Boer t curve (S_t) and from the hysteresis of the adsorption and desorption isotherm (S_{CUM}). The S_{BET} and S_{CUM} values were in good agreement. Some S_{BET} values are shown in Table I. It appeared that the t plots of sample S_8 and S_{13} yielded a negative intercept. This might be attributed to the organophilic nature of the silica surface. The standard t curve is valid for (hydr)oxide surfaces. For chemically different surfaces other t curves should be used (20). In none of the coated silica's an indication for ultramicropores was found.

2.3. Electron microscopy. From electron micrographs the size, shape, and size distribution of the particles were determined. In Fig. 4 the result is shown for three sam-

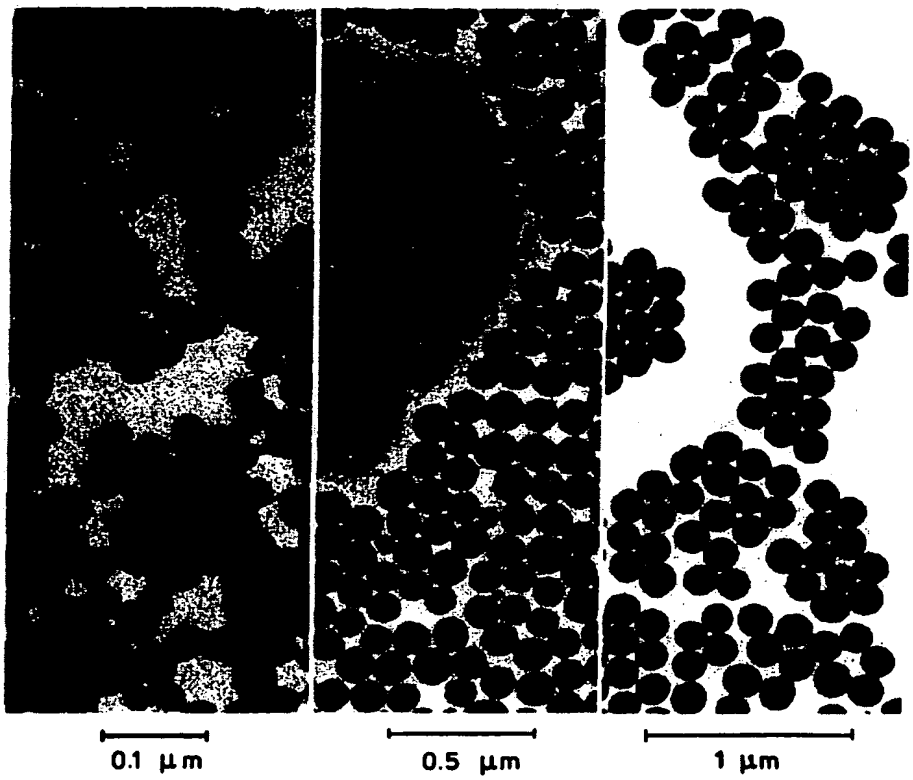

FIG. 4. Electron micrographs of samples S_8, S_7, and S_2 (from left to right).

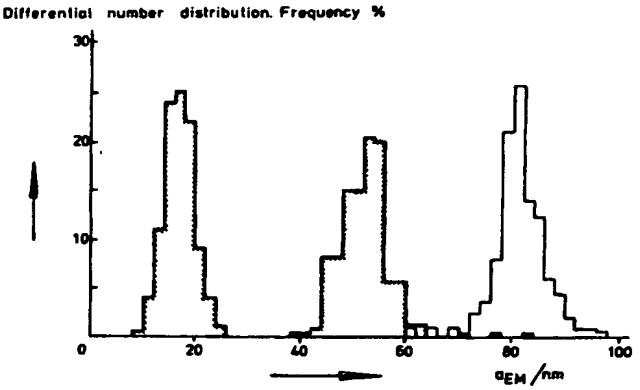

FIG. 5. Particle radius distribution data of S_8; ····, S_7; ---- and S_2; ——. The histograms are obtained from electron microscopy.

ples with increasing particle size. The spherical shape is well established for large particle sizes and the mean radius a_{EM} (number average) could be easily determined. For smaller particles (radius ≈ 20 nm) the particle shape is irregular. This might be an artifact, because the particles seem to be crowded by capillary forces upon evaporation of solvent. In solution the particles are probably more spherical. The size of the particles was determined by measuring $a_{EM} = \frac{1}{2}[a_1 b_1]^{1/2}$, a_1 and b_1 being the long and short axis of the particle. The size distribution is rather narrow (and symmetrical) for samples S_2 and S_7, but becomes relatively broader for smaller particle size, see Fig. 5. The results for the standard deviation are shown in Fig. 2. It can be seen from Fig. 2 that Δ does not change significantly after coating of the silica. We also investigated the influence of radiation intensity. First a very low intensity was used and the electronically amplified image was detected from a TV screen. Then the spot was radiated with a high dose and again an electronmicrograph was taken. All samples, which were measured showed a decrease in size upon intense radiation. Quantitative comparison for the small particles was difficult because of the low contrast of the particles. Samples S_2 and S_7 showed a shrinkage of approximately 5% in radius. This shrinkage, at least for S_2, cannot be satisfactorily explained by decomposition of the coating layer. It seems therefore that the silica structure itself shrinks as a result of radiation damage. This effect was also found for latex particles (21) and aluminum hydroxides (22). In Table II, a_{EM} values determined after intense radiation are presented.

TABLE II

Particle Size of Organophilic Silicas (in nm)

Sample	S_1	S_5	S_{10}	S_7	S_2
a_{EM}	16.5	16.7	21.5	53	81
a_D	22.0	23.1	26.5	62.5	91.5
a_{SAXS}	—	17.3	—	—	90
$a_{M_{ED}}$	19.4	20.8	24.1	65.2	—
$a_{S_{BET}}$	—	25.7	21.9	64.7	—
$a_{R_{ED}}$	27	27	—	63	97

2.4. Small-angle X-ray scattering. For samples S_2 and S_5, a SAXS experiment was performed. Values for a_{SAXS} are presented in Table II. The S_2 sample was dispersed in a mixture of cyclohexane and benzene (mole fraction benzene 0.65). The accuracy of the measurement of S_2 was limited because of particle sedimentation. The size distribution could not be determined. Sample S_5 was measured in cyclohexane. For S_5 the method of Vonk (16) could not be

applied since the size distribution appeared to be very narrow. Direct comparison of the experimental intensity curve with calculated intensity curves for different size distributions (log normal type) yielded a standard deviation in the radius of 6%.

2.5. Dynamic light scattering. Dynamic light-scattering measurements were carried out with dilute dispersions in cyclohexane. For sample S_5 measurements were also carried out in *n*-octane and diethylether. The autocorrelation function, $F(K, \tau)$ was determined for angles, $15° \leq \theta \leq 135°$. According to the theory (23) the autocorrelation function for the fluctuations in the scattered light of noninteracting particles is given by

$$F(K, \tau) \sim \exp(-\zeta\tau), \qquad [3]$$

where K is the wave vector, τ is the correlation time, $\zeta = 2D_0K^2$, where D_0 is the diffusion coefficient. For each K the logarithm of the autocorrelation function was fitted with a quadratic function in τ, and D_0 was found according to the usual cumulant method. For dilute dispersions the hydrodynamic radius, a_D, is related to D_0 by the Stokes–Einstein law,

$$D_0 = k_BT/6\pi\eta a_D, \qquad [4]$$

where k_B is the Boltzmann constant, T the absolute temperature, and η is the viscosity of the medium.

The value of D_0, measured at different angles, was slightly smaller for low values of scattering angle, θ. In Table I average D_0 values are listed, which are determined by taking the best linear fit in a ζ versus K^2 plot. As a result of this procedure the average D_0 is mainly determined by the scattering at higher angles. The results for S_5 in *n*-octane and diethylether are compiled in Table III.

2.6. Sedimentation. Sedimentation measurements were performed with dilute dispersions in cyclohexane (S_3, S_5, S_7), in *n*-octane and diethylether (S_5) and in *n*-heptane (S_{13}). The results are presented in Tables I and III. The molar mass M_{SD} of the particle can be calculated from the diffusion coefficient, the sedimentation coefficient, s_0, and the specific volume, $\bar{v}$ ($=\delta^{-1}$), of the particle (measured in cyclohexane) according to

$$M_{SD} = s_0RT/D_0(1 - \bar{v}\delta_0), \qquad [5]$$

where R is the gas constant, δ_0 is the density of the solvent. Data for δ_0 were taken from the literature (24).

2.7.1. Static light scattering. Static light-scattering experiments with S_3 dispersions in cyclohexane and chloroform were done with dilute as well as concentrated solutions (4, 5). It appeared that at very low concentration, $c < 10^{-2}$ g cm^{-3}, a relatively large second virial coefficient was measured. In order to investigate the light-scattering behavior of very dilute silica dispersions more accurately, dispersions of S_5 in cyclohexane, *n*-octane, and diethylether were measured. The refractive index increments were experimentally measured in cyclohexane ($14.6 * 10^{-3}$ cm^3 g^{-1}) and in diethylether ($= 70 * 10^{-3}$ cm^3 g^{-1}), both for $\lambda_0 = 436$ nm. The value of dn/dc in *n*-octane was calculated from the value in cyclohexane with the Wiener equation. The results were interpreted according to Eq. [1]. Zimm plots are shown in Fig. 6 for cyclohexane and *n*-octane ($\lambda_0 = 436$ nm). The re-

TABLE III

Characterization of S_5 in Very Dilute Dispersions, $C < 11 \times 10^{-3}$ g cm^{-3}

	Cyclohexane	*n*-Octane	Diethylether
$M/10^7$ g mole^{-1}	4.8	4.4	—
A_2/cm^3 g^{-1}	13	14	—
R_g/nm	22	24	—
$D_0/10^{-11}$ m^2 sec^{-1}	1.05	1.82	2.9
$s_0/10^{-10}$ sec	0.84	1.50	3.5
$M_{SD}/10^7$ g mole^{-1} [a]	3.7	3.7	5.3

[a] Calculated according to Eq. [5] with $\bar{v} = 0.609$ cm^3 g^{-1}.

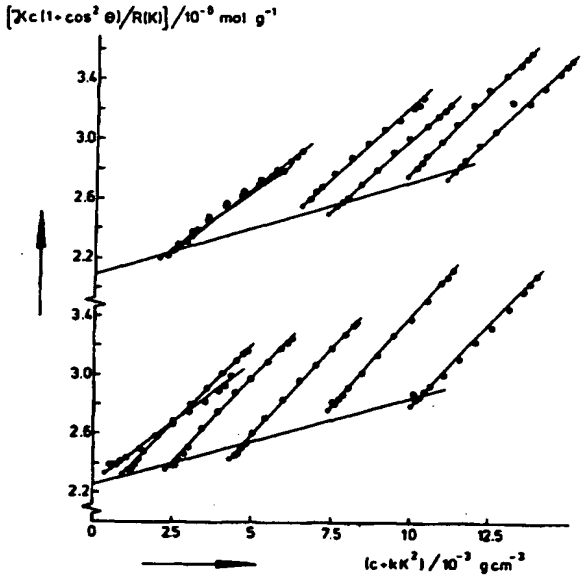

FIG. 6. Zimm plots of S_8 in cyclohexane (⊗) and in *n*-octane (⊙). $k = 2.5 \times 10^{-14}$ g cm^{-1}, $\lambda_0 = 436$ nm, ●, are $K^2 \to 0$ extrapolated points.

sults for $\lambda_0 = 546$ nm were similar. Data for M, A_2, and R_g are presented in Table III.

The experiments in diethylether show a complex behavior. At small concentrations maxima in the scattering intensity are found, see Fig. 7. At higher angles the angular dependence is linear at the lowest concentration but curved at higher concentration. We

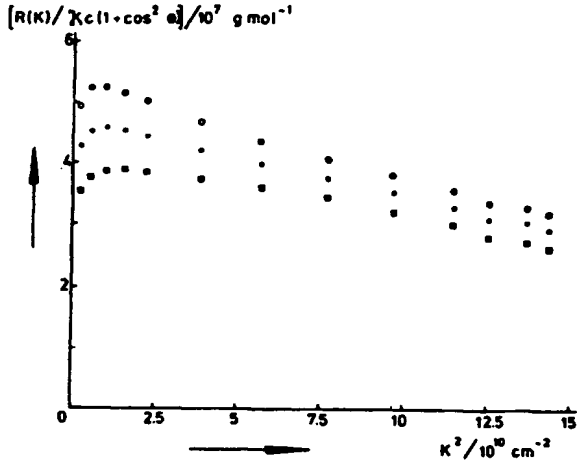

FIG. 7. Scattering curves of S_8 in diethylether: ○, $c = 1.3$ g dm^{-3}; ●, $c = 2.1$ g dm^{-3}; □, $c = 4.7$ g dm^{-3}; $\lambda_0 = 436$ nm.

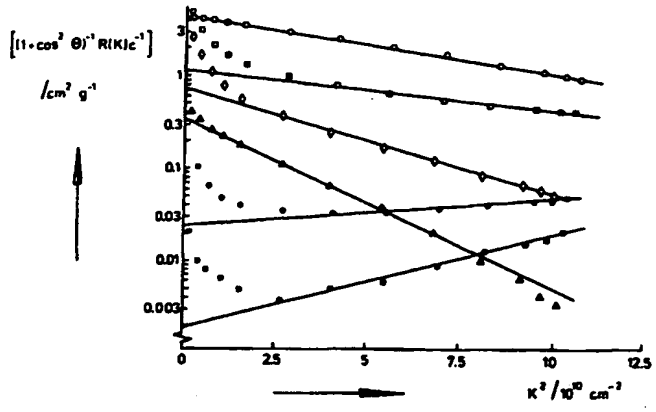

FIG. 8. Guinier plots of light scattering results of S_2 dispersions in mixtures of cyclohexane and benzene (λ_0 = 546 nm). The particle concentration is approximately 3.5×10^{-3} g cm^{-3}. The mole fraction benzene is ◇, 0.00; △, 0.20; ■, 0.26; ●, 0.33; □, 0.49; ○, 0.65.

think that in diethylether strong electrostatic interaction occurs, giving rise to long range ordering of the particles (25). However, also in cyclohexane and *n*-octane where the Zimm plots are regular we expect that the large value of A_2 is due to electrostatic interaction although less strong than in diethylether.

2.7.2. Static light scattering. Contrast variation. With some dispersions we performed contrast variation experiments. The scattering power of the system is varied by changing the dispersion medium. Application of this method to conventional light scattering with S_7 dispersions in cyclohexane–*trans*-decaline mixtures was previously reported (4). Here we shall give some results with S_2 and S_3 (in mixtures of cyclohexane–benzene) and S_5 (in mixtures of cyclohexane–*trans*-decaline), together with the earlier reported S_7 data. As an example the scattering intensity as a function of K^2 is shown in Fig. 8 (sample S_2). The curvature of the angular dependence in the low K^2 region reflects the presence of small amounts of clustered particles (4). The results measured at high angles and extrapolated to $K = 0$ from high angles are interpreted according to Eqs. [6] and [7] derived in (4),

$$n_0^{-1}(R(K=0)/2C)^{1/2} = (2\pi^2 M_{CV}/\lambda_0^4 N_A \delta^2)^{1/2}(\bar{n}_p - n_0), \quad [6]$$

$$R_g^2 = R_{g0}^2 + E(\bar{n}_p - n_0)^{-1}, \quad [7]$$

where $\bar{n}_p$ and n_0 are the (mean) refractive indices of particle and medium, M_{CV} is the molar particle mass (the subscript indicates determined with contrast variation), δ is the density of the particles, R_{g0} is the radius of gyration of the equivalent homogeneous particle, and E is a measure of optical density fluctuations within the particle.

As can be seen from Eq. [6], $\bar{n}_p$ and M_{CV} can be determined from a plot of $n_0^{-1}(R(K=0)/2C)^{1/2}$ versus n_0 when δ is known. In Fig. 9 such a plot is shown for S_2. There is quite a discrepancy in $\bar{n}_p$ and M_{CV} values of S_2. The difference in slope between series 1 and series 2 and 3 might be caused either by a different dispersion preparation or by aging of the silica. Series 1 was prepared by dispersing the silica in previously mixed solvents. Series 2 and 3 were prepared by dispersing the silica in pure cyclohexane and diluting the sol with benzene. Series 2 and 3 were measured after dry storage of the particles for at least 3 months.

According to Eq. [7], R_{g0} and E can be

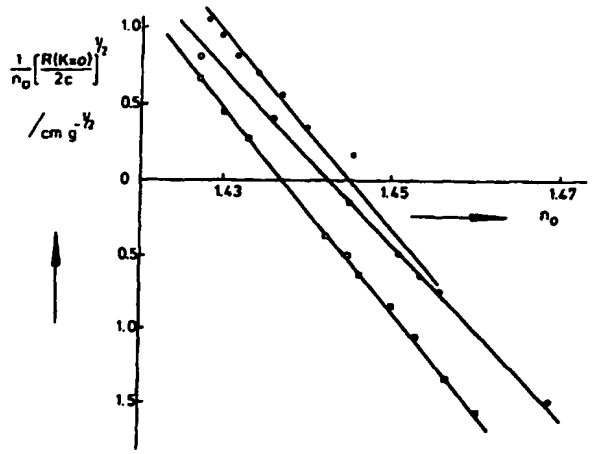

FIG. 9. Square root of the scattering intensity at zero angle for S_3 dispersions in cyclohexane-benzene mixtures (λ_0 = 546 nm). ○, 1st series; ●, 2nd series, □, 3rd series.

obtained by plotting R_g^2 versus $(\tilde{n}_p - n_0)^{-1}$. For S_2 we found a linear dependence for each series with different $\tilde{n}_p$ yielding approximately the same R_{g0} and E values. For S_3 and S_5 the experimental data were rather scattered and no E values could be determined. Apparently the particle size is too small to perceive optical density fluctuations accurately.

IV. DISCUSSION

1. Preparation

Alcosols can be prepared without difficulty in a rather reproducible manner. A critical step is the coating reaction. The silica changes from hydrophilic to hydrophobic and precautions must be taken to avoid irreversible aggregation of silica particles in the intermediate stage. Such an irreversible aggregation by siloxane-bridge formation between different particles is known from literature (8). It is important to keep the water concentration as low as possible just before the esterification reaction, because siloxane-bridge formation is retarded in a nonaqueous medium. It seems also expedient to keep the concentration of silica particles in the melt of the alcohol reagent not too high, in order to minimize interparticle contacts. This can be accomplished by adding sufficient stearyl alcohol.

Although laborious, the purification of organophilic silica from excess stearyl alcohol by ultracentrifugation is satisfactory for particles with radius larger than 50 nm. For smaller particles the centrifugation speed and/or time becomes large and the resulting sediment of silica is difficult to redisperse again as individual particles. The nitrogen flow distillation seems an unattractive alternative, because drying the silica at high temperatures might also promote aggregation. Further work has to be done to find a better manageable purification procedure.

2. Characterization Techniques

Now we shall compare the particle size values, either directly measured with or calculated from different techniques, see Table II. Each method yields a different average of the particle size distribution. This effect is small, however, since the polydispersity is small for all samples. Hydrodynamic radii, a_D, were calculated from diffusion coeffi-

cients according Eq. [4]. From the molar mass, M_{SD}, and the particle density, $a_{M_{SD}}$, is calculated $a_{M_{SD}} = (3M_{SD}/4\pi\delta N_A)^{1/3}$. From the radius of gyration of the equivalent homogeneous particle $a_{R_{g0}}$ is obtained; $a_{R_{g0}} = (5/3)^{1/2}R_{g0}$. Also from the surface area S_{BET} and the particle density the particle size can be determined: $a_{S_{BET}} = 3/S_{BET}\delta$. The electron microscopy results appeared to be quite small even when corrected for shrinkage (approximately 5%). Also SAXS yields rather low values, but one should recall that the electron density difference between solvent and organophilic layer is negligible, rendering the coating layer invisible. Hydrodynamic radii are expected to be largest, since they also measure solvent "bound" to the particle surface. $a_{M_{SD}}$ should lie between a_D and a_{SAXS}, because the density used to calculate $a_{M_{SD}}$ is an average value of silica core and organophilic layer. $a_{R_{g0}}$ yield too large values especially for small particle sizes. We think this results from some (limited) aggregation (doublets etc.), which has been reported earlier (5).

3. *Particle Structure*

From the carbon content the weight percentage stearyl chains can be calculated, assuming that all carbon originates from stearyl chains. The associated hydrogen is then calculated and subtracted from the percentage hydrogen in Table I. The remaining hydrogen is attributed to water present as silanol and water possibly trapped in the particles during their preparation. The percentage of silica is calculated from the silicon content. The sum of the percentages in Table IV do not precisely add up to 100 due to small errors in the analyses probably that of hydrogen. The density of the silica core, δ_{core}, can be calculated from the density of the total particle (see Table I) and of the layer and the weight percentage of the layer. We took $\delta_{layer} = 0.77$ g cm^{-3} equal to liquid alkane chains. Similarly the refractive index of the silica core, n_{core}, was calculated according the equation of Arago and Biot (e.g., 27), that can be applied since $n_{core} \simeq n_{layer}$. By extrapolation of the refractive indices of homologous alkanes we found $n_{layer} = 1.438$ for $\lambda_0 = 546$ nm. The density and the refractive index of the silica core tend to decrease with increasing particle size, see Table IV. The appreciable water content, low density, and low refractive index indicate an amorphous silica structure. This is also confirmed by particle shrinkage in electron microscopy, and for the alcosol particles by the ultramicropores found with surface area measurements. Comparison of S_5^* ($\delta = 1.87$ g cm^{-3}) and S_5 ($\delta_{core} = 2.10$ g cm^{-3}) shows that the silica of the coated particles is more compact. High E values for S_7 and S_2 indicate that the periphery of the silica core is more compact than the interior of the particle (4).

These phenomena as well as the decreasing density and refractive index with in-

TABLE IV

Calculated Results from CH Analyses, and Refractive Index and Density Measurements

	S_0	S_5	S_{22}	S_7	S_2
Stearyl chains/% (w/w)[a]	17.8	15.8	15.3	7.4	3.4
Water/% (w/w)	8.6	7.9	4.6	7.4	10.8
SiO_2/% (w/w)	76.4	79.3	79.2	85.8	—
δ_{core}/g cm^{-3}	2.13	2.10	2.26	1.99	1.89[b]
n_{core} ($\lambda_0 = 546$ nm)	1.462	1.455	—	1.440	1.442
Coverage/nm^2 chain^{-1}	—	0.20	0.23	0.15	—

[a] Calculated as distearyl ether.
[b] Density of S_2 is assumed $\delta = 1.80$ g cm^{-3}.

creasing particle size can be qualitatively explained. Iler (8) suggested that the silica particles obtained by Stöber *et al.* (7) were formed by uniform aggregation of much smaller ultimate particles less than 5 nm in size. Our SAXS results of alcosols as well as the observed ultramicroporosity corroborate this suggestion. McMillan (28) found that the porosity of inner and outer regions of the particles could be changed depending on the reaction conditions. Freshly made particles obtained at 25°C were highly porous to nitrogen. Upon heating at 90°C the area determined with nitrogen strongly decreased. In both cases, however, the area determined with OH^- ions was the same. This indicates that upon heating the diameter of the peripheral pores decreases so that nitrogen could not penetrate. By heating the sol for a longer time at pH 10 the pores close further and some water is trapped inside. It seems likely that such siloxane-bridge formation also occurs upon evaporating the ethanol and during the coating reaction. At the periphery of the particle the water which is formed can escape leaving a compact silica structure. For (the interior of) relatively large particles, however, this becomes increasingly difficult. As a result the mean density of large particles is lower and the density variation larger.

The silica surface is covered with stearyl chains. This is evident from the good organophilic properties and the carbon content of coated particles. Straightforward calculation of the surface coverage from the weight percentage stearyl chains and the surface area yields high values compared to the value reported by Ballard (15), 0.37 nm^2/chain, see Table IV. The figure for S_7 is even lower than the closest packing value (=0.21 nm^2) for aliphatic chains (29). The discrepancy is explained by the surface roughness of the alcosol particle. Assuming the ultimate particles forming the silica particle are 2 nm in size (see Fig. 3), it follows that the real surface is approximately two times larger than the geometric surface area. Taking into account this correction factor, reasonable agreement exists between the value of Ballard and our results.

Alcosol particles are stabilized by electrostatic repulsion. The charge originates from silanol groups, which are relatively acid and dissociate in the presence of ammonia. During the coating reaction the charge density sharply decreases, because ammonia is evaporated and the particles are brought in a much less polar medium. When dispersed in diethylether again electrostatic repulsion dominates the particle interactions. In aliphatic solvents only very little charge can produce a considerable potential, which is hardly screened in the medium due to the low concentration of ions. These long range interactions were measured in cyclohexane and *n*-octane at very low particle concentrations. At higher concentrations short range hard repulsions dominate (5). Albers and Overbeek (30) explained that at high concentrations the gradient of the potential becomes small since the particles are close together. In view of this we can understand that electrostatic interactions are negligible at high concentrations.

We conclude that stable organophilic silica dispersions can be prepared with particle radius between 20 and 100 nm and narrow size distribution. The amorphous silica can be coated with a dense layer of aliphatic chains rendering it organophilic. Characterization results can be qualitatively explained in terms of an initially porous alcosol particle, which is dehydrated to some extent in the coating reaction. Surprising was the electrostatic repulsion in aliphatic solvents at low concentrations.

ACKNOWLEDGMENTS

The authors wish to acknowledge Mr. H. Mos for performing dynamic light-scattering experiments, Mr. J. Suurmond for conducting ultracentrifugation experiments and Mr. J. Pieters for conducting electronmicroscopy experiments. Mr. P. Elberse and Mr. A. C. Vermeulen are thanked for carrying out nitrogen adsorption experiments and for helping with interpretation. We are debtful to Dr. P. van Hutten, State

University of Groningen, and Dr. C. Vonk, D. S. M. Geleen, for performing and interpreting SAXS experiments. We thank Mr. H. de Hek and Prof. P. L. de Bruyn for critically reading the manuscript, Mr. W. A. den Hartog for the illustrations, and Mrs. M. Uit de Bulten for typing the manuscript.

REFERENCES

1. Vrij, A., Nieuwenhuis, E. A., Fijnaut, H. M., and Agterof, W. G. M., *Discuss. Faraday Soc.* **65**, 101 (1978).
2. Nieuwenhuis, E. A., and Vrij, A., *J. Colloid Interface Sci.* **72**, 321 (1979).
3. Agterof, W. G. M., Van Zomeren, J. A. J., and Vrij, A., *Chem. Phys. Lett.* **43**, 363 (1976).
4. van Helden, A. K., and Vrij, A., *J. Colloid Interface Sci.* **76**, 418 (1980).
5. van Helden, A. K., and Vrij, A., *J. Colloid Interface Sci.* **78**, 312 (1980).
6. Matijević, E., *Progr. Colloid Polym. Sci.* **61**, 24 (1976).
7. Stöber, W., Fink, A., and Bohn, E., *J. Colloid Interface Sci.* **26**, 62 (1968).
8. Iler, R. K., "The Chemistry of Silica." Wiley, New York, 1979.
9. Boksanyi, L., Liardon, O., and Kovats, E., *Advan. Colloid Interface Sci.* **6**, 95 (1976).
10. Papirer, E., Morawski, J. C., and Vidal, A., *Angew. Makromol. Chem.* **42**, 91 (1975).
11. Laible, R., and Hamann, K., *Advan. Colloid Interface Sci.* **13**, 65 (1980).
12. Deuel, H., Wartmann, J., Hutschnecker, K., Schobiner, U., and Güdel, C., *Helv. Chim. Acta* **42**, 1160 (1959).
13. Iler, R. K., *Surface and Colloid Sci.* **6**, 77 (1973).
14. Iler, R. K., U. S. Patent 2,601,185.
15. Ballard, C. C., Broge, E. C., Iler, R. K., St. John, D. S., and McWhorther, J. R., *J. Phys. Chem.* **65**, 20 (1961).
16. Vonk, C. G., *J. Appl. Cryst.* **9**, 433 (1976).
17. de Boer, J. H., Linsen, B. G., and Osinga, Th. J., *J. Catal.* **4**, 643 (1965).
18. Wheeler, A., "Catalysis," Vol. II, Chap. 2. Rheinhold Publ. Corp, New York, 1955.
19. Kerker, M., "The Scattering of Light and Other Electromagnetic Radiation." Academic Press, New York, 1969.
20. Lecloux, A., and Pirard, J. P., *J. Colloid Interface Sci.* **70**, 265 (1979).
21. McDonald, S., Daniels, C., and Davidson, J., *J. Colloid Interface Sci.* **59**, 342 (1977).
22. Catone, D. L., and Matijević, E., *J. Colloid Interface Sci.* **48**, 291 (1974).
23. Berne, B. J., and Pecora, R., "Dynamic Light Scattering." Wiley, New York, 1976.
24. Johnson, B. L., and Smith, J., *in* "Light Scattering from Polymer Solutions" (M. D. Hughlin, Ed.). Academic Press, London, 1972.
25. Doty, P., and Steiner, R. F., *J. Chem. Phys.* **19**, 774 (1951).
26. Davydov, V. Y., Kiseler, A. V., and Zhuravlev, L. T., *Trans. Faraday Soc.* **60**, 2254 (1964).
27. Heller, W., *J. Phys. Chem.* **69**, 1123 (1965).
28. McMillan, D., U. S. Patent 3591518 (1971).
29. Rabinovitch, W., Robertson, R. F., and Mason, S. G., *Canad. J. Chem.* **38**, 1881 (1960).
30. Albers, W., and Overbeek, J. Th. G., *J. Colloid Interface Sci.* **14**, 501 (1959); ibid. **14**, 510 (1959).
31. Kops-Werkhoven, M. M., and Fijnaut, H. M., *J. Chem. Phys.*, in press.